# Electromyography-based Forearm Prosthetic

David Hoang[1], Felix Cruz[1], Naseem Ali[1], Vanessa Cini[1], and Zach Ermert[1]

***Abstract*— Functionality is an essential aspect of prosthetics as many people with missing limbs find difficulty in adapting to the standards of everyday tasks. Prosthetics have greatly encouraged people with missing limbs to feel more confident and strive through difficult activities, but there is still much more room for improvement. In hopes of creating a compatible prosthetic, we designed and analyzed a circuit that could help bring functionality to an EMG-based prosthetic hand connected to the flexor carpi radialis and extensor carpi radialis. We aimed to achieve an overall gain of 160 and a frequency range of 20-500 Hz. Our design utilizes buffers and an instrumentation amplifier that leads to second order high and low pass filters to filter out noise outside of 20Hz and 500Hz, followed by a non-inverting amplifier to increase the overall gain. By testing our system using the Java applet Falstad and graphing a bode plot, we confirmed that our calculated frequencies and voltages fulfilled our required design measurements. Overall, through use of functional engineering analysis and bioinstrumentation techniques, we were able to effectively produce the framework behind an EMG-based prosthetic system for an amputee forearm, whereby further hands-on simulation would provide a better measure of functionality and transparency for clinical use.**

## I. Introduction

### A. Motivation

Developments in prosthetic technology over recent years has been attributed to increasing amputation rates around the world. In the United States alone, there were reported to have been nearly 2 million people with missing limbs, whereby this number is projected to double by the year 2050 [1]. Numerous physical and psychological impairments commonly associated with amputations include the likes of phantom-limb pain sensations, post-amputation depression, maladaptive coping styles, mutilation anxiety, muscle fatigue, and shortened livelihoods [2]. In order to mitigate the potentiality for these side effects and to improve amputees' overall wellbeing, the importance for proper rehabilitation methods has stimulated a high clinical demand for prosthetic intervention. So, to better enhance the performance of everyday activities, upper extremity prosthetics have been widely regarded for clinical application. Thus, through electromyography (EMG)-based technology, artificial forearm prostheses can be designed to strengthen cognitive motor controls over the coordination of nervous and musculoskeletal systems.

### B. Solution Overview

Modern myoelectric prostheses generally integrate input signal acquisition units, processing and control units, and surface EMG signal-controlled end effectors [3]. Using scientific-based assumptions backed by academic literature, we were able to systematically model an EMG-based forearm prosthetic through the implementation of multiple active circuit components, with an instrumentation amplifier and bandpass filter being key components. The scope of the circuit is limited to the detection and basic processing of an input signal, with an analog-to-digital converter being the last component of our design. Thus, digital processing is not considered in this study. To design a functional system, we deduced that specifications must include the capability to accurately detect muscle contractions while simultaneously filtering out interfering noise, as well as the proficiency to amplify rather small signals to increase detectability.

### C. Aim of study

In this study, we aimed to design and analyze a circuit that would successfully filter and amplify biological signals located in the forearm muscles. Furthermore, we discuss potential applications of an EMG-based prosthetic as a whole and consider future steps to take towards realizing a more extensive design.

## II. Methods

### A. Determining Parameters

Our design parameters were mainly determined by looking at pre-existing literature and research. First, we assumed that patients would have a functioning forearm, and thus chose muscles in the forearm region. We focused on the flexor carpi radialis and extensor carpi radialis as the muscles of interest for our electrode placements. Further research into EMG signals and these specific muscles found that the typical voltage range would be 1-10 mV. Since various studies used different frequency ranges, we chose a range that was most common among our sources: 20-500 Hz [3], [7].

In our design, we also assumed that the circuit was powered by a 3.3 V battery, all op-amps were ideal and that resistors in the instrumentation amplifier had a tolerance of 1 percent.

### B. Virtual Design

Our design can be broken down into five key stages: 1) electrodes and buffers, 2) instrumentation amplifier, 3) Sallen-key bandpass filter, 4) a non-inverting amplifier, and 5) an analog-to-digital converter (ADC) as shown in Fig. 1. We used an online circuit diagrammer, Partsim, in order to draw an initial sketch of our design.

[1]Department of Bioengineering, Jacobs School of Engineering, and Institute for Neural Computation, UC San Diego, La Jolla, CA 92093, USA.

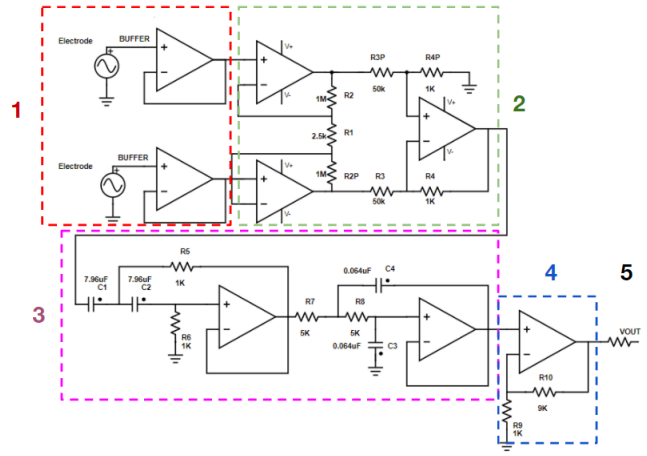


Fig. 1. Overview of the circuit design. 1). Electrodes modeled as AC inputs followed by buffers. 2). Instrumentation amplifier. 3). Active bandpass filter composed of a high pass filter followed by a low pass filter. 4). Non-inverting amplifier. 5). Output leads to an ADC.

*1) Electrodes and buffers:* First, the electrodes serve as the point of contact between the forearm skin and the circuit. As opposed to the commonly used Ag/AgCl electrodes, we decided to integrate orbital electrodes into our design. The reason behind this choice was the fact that Ag/AgCl electrodes deteriorate with time from their interaction with sweat. In a home-patient setting, this is non-ideal as it necessitates frequent in patient visits for electrode update and replacement. Dry orbital electrodes therefore provide an attractive alternative to Ag/AgCl electrodes since they are more durable and longer lasting. This claim is further substantiated by the fact that orbital electrodes have comparable electrode-skin impedances to Ag/AgCl electrodes, which is important in maintaining signal quality. Orbital electrodes have low electrode-skin impedances due to their unique shape, which permits large contact area with the skin. Of particular interest are its pins which penetrate the stratum corneum layer of the skin and improve the detection of biopotentials within the body [5].

Following the electrodes are buffers, which serve to prevent drawing too much current from the electrodes. Since buffers prevent loading in between stages, they prohibit the circuit from overheating and maintain a smooth electrical transition from electrode to differential amplifier.

*2) Instrumentation Amplifier:* Due to the differential input signal, an instrumentation amplifier was used. The instrumentation amplifier is useful for many reasons, the most important being reduction of common-mode interference. As the term suggests, common-mode interference appears with equal strength at all terminals, hence "common". Elimination of common-mode noise is done through a differential instrument with differential gain, effectively subtracting out the common-mode component. The efficacy of the instrument in removing common-mode gain is reflected through the common-mode rejection ratio (CMRR), which can be defined as the ratio of the differential gain over the common mode gain [6]:

$$CMRR_{db} = 20log_{10}(\frac{|A_d|}{|A_c|}) \quad (1)$$

where Ad, the differential gain, and Ac, the common-mode gain, are defined as

$$A_d = (1 + 2\frac{R_2}{R_1})(\frac{R_4}{R_3}), A_c = 0.04(\frac{R_4}{R_3}) \quad (2)$$

Typically, an effective CMRR is at least 80 db. Thus, we designed our instrumentation amplifier to have a CMRR of 86.03 dB, where the differential gain was 16.02 and the common-mode gain was $8x10^{-4}$. This was achieved with resistive values of

$$R_1 = 2.5k\Omega, R_2 = 1M\Omega, R_3 = 50k\Omega, R_4 = 1k\Omega$$

Aside from eliminating noise, the instrumentation amplifier is also useful for accounting for tolerance sensitivity in resistive values and provides a high input impedance [6].

*3) Sallen-Key bandpass filter:* A Sallen Key bandpass filter was chosen to ensure that the biological signals of interest were relatively free of noise and within our predetermined frequency range of 20 to 500 Hz. In the case of EMGs, a typical frequency range is between 0 and 500 Hz; however, research indicates that the most useful frequency range for signal data acquisition is found between 50 and 150 Hz [7]. Despite this fact, this report focuses on capturing the 20 to 500 Hz range to better represent and include the biological signals that may be considered noise, warranting the need for a bandpass filter. The following cut-off frequency equation was used:

$$\omega = 2\pi f = \frac{1}{RC} \quad (3)$$

which is valid when $R_1 = R_2$ and $C_1 = C_2$.

Assuming a critically damped output, we chose appropriate R and C values that would yield our desired cut-off frequencies and fit our established design constraints. In the case of the low pass filter, a R value of 1kΩ and C value of 7.9577$\mu$F was chosen. For the high pass filter, a R value of 5kΩ and C value of 0.064$\mu$F was used. Fig. 2 represents the resulting bode plot with these parameters and includes vertical black lines that depict the calculated cut off frequencies (125.7 and 3141.6 in rad/s). An additional design decision that was made was ensuring that this filter stage had unity gain, a gain of 1, in order to better control the overall gain of the input signal with the non-inverting amplifier that proceeds.

*4) Non-inverting Amplifier:* A non-inverting operational amplifier was chosen to be the final stage of the design before the ADC to provide the circuit with a large enough signal for data acquisition readings and analysis. Seeing as the previous filter stage had unity gain, an additional amplification of the signal was implemented to bring the overall gain of the circuit to 160.2 using resistance values of 1kΩ and 9kΩ, creating a gain of 10 in this particular section and increasing the gain from the instrumentation

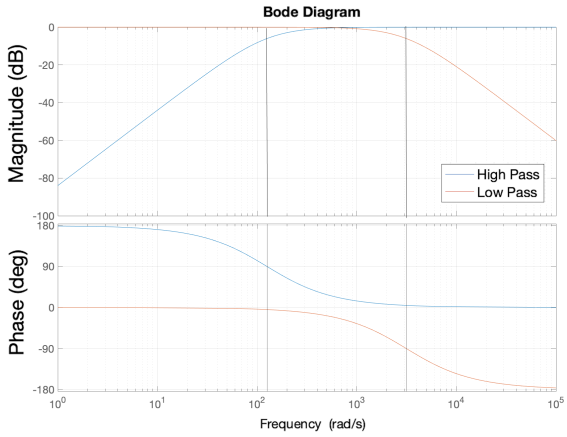


Fig. 2. Bode plot containing behavior of both the high pass filter (blue) and low pass filter (orange). Cut-off frequencies are denoted with a vertical line at 125.7 and 3141.6 rad/s, indicating roll-off points for signals outside of range.

amplifier in a multiplicative fashion. Designing circuits with the appropriate gain is crucial in analyzing biological signals which are naturally weaker and in need of amplification to implement them in a variety of medical devices and experiments.

*5) Analog-to-digital Converter:* Although it is not explicitly shown in our diagrams, an analog-to-digital converter is the intended recipient of the amplifier output. An ADC allows us to convert the voltage signal from the output into a digital format, which can subsequently be read by a digital controller to operate the prosthetic arm. While the digital aspect is outside of the scope of our design, the ADC is an important component in ensuring that the signals going through our circuit can be read. In this case, since our theoretical output range is around 1.44V (theoretical input range times gain), a 10-bit ADC would allow for a resolution of around 1.4 mV. This is a sufficient resolution to detect changes in input strength.

### C. Circuit Simulation

The circuit design was simulated using the online Java applet Falstad. Using the applet, six different input frequencies were tested: 1Hz, 20Hz, 150Hz, 300Hz, 500Hz, and 10kHz. The maximum voltage was set to 10mV, based on our initial design parameters, and the input type was set to AC. The applet includes a feature that graphs output voltage over time, which we used to observe the behavior of our design. Based on the input frequency, the time step was automatically adjusted by the program. The op-amps are simulated to be ideal, and all capacitors have an initial voltage of 0V.

## III. Results

The simulation in Falstad yielded the voltage graphs pshown in Fig. 3. At frequencies within the bandwidth (150 Hz and 300 Hz), we observed a normal oscillatory signal characteristic of the AC input signal. The maximum voltage for both frequencies was 1.267 V and 1.050 V, respectively. Frequencies at the border of the bandwidth range (20Hz, 500Hz) also showed regular oscillatory signals, but with maximum voltage magnitudes of 700mV. With a 1 Hz input, repeated spike-like patterns were observed with small magnitudes of 18 mV, the most prominent peak of 29.166 mV occurring at the very start of the simulation. Similarly, at a 10kHz input, a large spike of 30.55 mV was observed at the beginning followed by small oscillations of 2.7 mV, appearing as a bold line given the timescale of the graph.

## IV. Discussion

### A. Simulation Analysis

Given the fact that the tested frequencies of 150 Hz and 300 Hz both yielded normal oscillations, it is safe to assume that the bandwidth filter allows frequencies well within the 20 - 500 Hz range to pass through without affecting the signal integrity. It is interesting to note that while the theoretical gain was 160, the output magnitudes of 1.267 V and 1.050 V, respectively, were representative of gains slightly less than 160. At 20 Hz and 500 Hz, we observe the expected drop-off behavior of a bandpass filter. Although the oscillatory signals were maintained, the peak voltages were 775 mV and 731 mV, respectively. As illustrated in the bode diagram (Fig. 2), the signal magnitude is expected to start dropping at these cutoff points. At 1 Hz and 10 kHz, the attenuation and filtering of signals outside of the bandwidth range is clear. Though we cannot currently determine the cause of the signal behavior at 1 Hz, the peak magnitude of 18 mV is small enough in comparison to the peak magnitudes of signals within the bandwidth range. Similarly, we can actually see a critical damping effect in the graph for 10 kHz, which starts with a large spike and continues to diminish to small oscillations at peak voltages of around 2.7 mV. Thus, we can conclude that signals outside our target range can be filtered out, while amplifying target signals close to our desired gain.

### B. Benefits and Drawbacks

The design of our circuit is beneficial to the wearer in several important ways. First, due to the noise-minimizing effect by the instrumentation amplifier, the patient would be unrestrained in their daily activities or interactions around other electrical appliances and devices which would prevent disruption of the prosthetic's functionality. The other benefit is the durability of the orbital electrodes that are integrated into the circuit, which achieve a low-electrode skin impedance due to their design. The selection of an appropriate bandwidth between 20-500 Hz will ensure noise minimization from skin potentials and other external interference, enabling a clear reading of the signals of interest. However, there are also some drawbacks to take into consideration. Biopotential signals vary from person to person, which could require a more specific and personalized circuit for the patient. Patients wearing this prosthetic would also be limited in certain movements, because of the failure of extrinsic muscle signals to detect certain postures. For instance, the extrinsic muscle, which remains mostly intact in partial hand amputees, may be used for conventional myoelectric prosthesis control, but

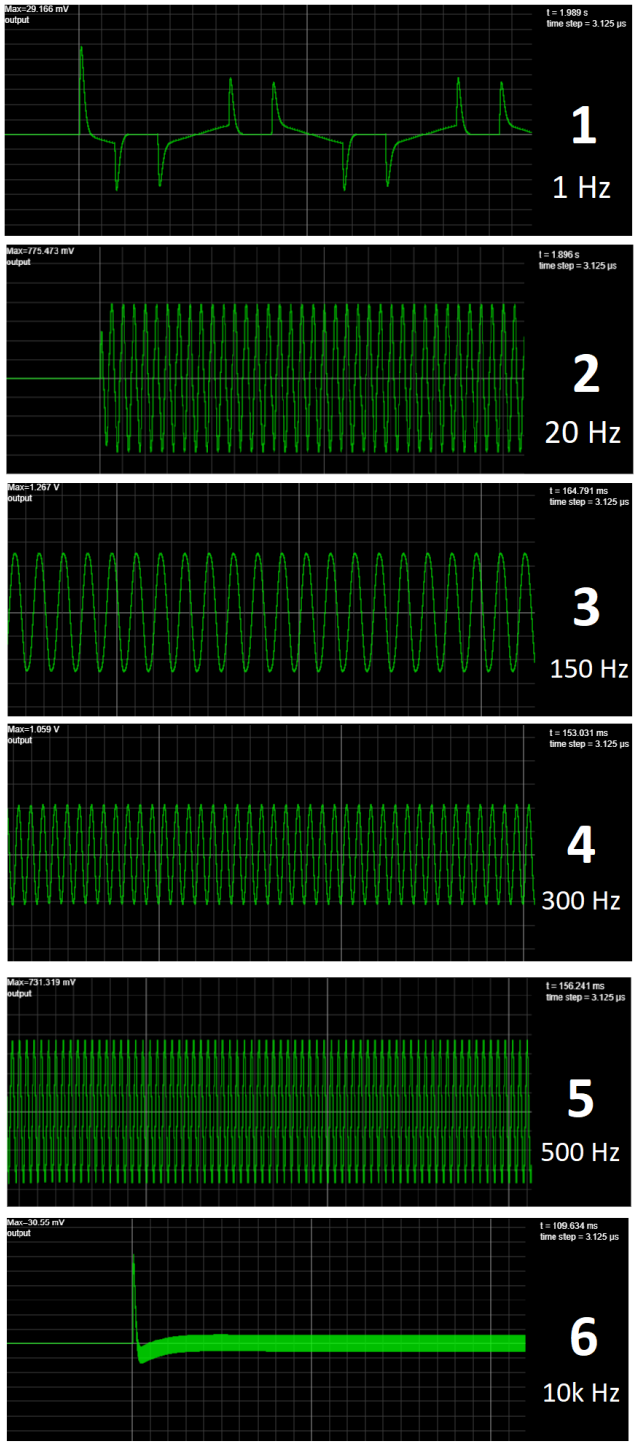


Fig. 3. Result of simulation in Falstad. 1). 1 Hz with 100 ms/div. 2). 20 Hz with 100 ms/div. 3). 150 Hz with 5 ms/dv. 4). 300 Hz with 5 ms/div. 5). 500 Hz with 5 ms/div. 6). 10kHz with 5 ms/div. Normal oscillations can be seen in plots 2-5, with attenuation occurring in 6 and low amplitudes occurring in 1 and 6.

in doing so would compromise normal wrist movement and limit hand function [4]. The last drawback to consider is skin movement beneath the electrode, potentially causing unwanted artificial motion.

### C. Future steps

Moving forward with our design, we would like to implement methods of patient protection, such as preventing shock and thermal hazards. Some possibilities would be to test an earth-to-ground connection in reducing shock hazard, as well as protective resistors and diodes in case of shorting. To minimize the risk of thermal hazard, we can cover resistive elements of the circuit with protective casing and introduce a circuit breaker to circumvent thermal overload. Ultimately, we would like to explore beyond the ADC and consider aspects of the digital format, allowing the signal to be readable by the prosthetic arm and better benefit its functionality. Some factors to consider for digital conversion are the sampling rate, quantization, and a range of conversion.

## ACKNOWLEDGMENTS

We would like to express our gratitude to Professor Cauwenberghs for his time and dedication in instructing this quarter. The course, although challenging, was very intriguing, thought-provoking, and full of valuable knowledge for future bioengineers. We are especially grateful for the various instances of understanding from the professor with respect to homework deadlines. Lastly, a big thanks to Anuja, Preston, and Qin for their help on class concepts and the homework during office hours and discussions. The help of the TA's were essential to understanding and completing this course.

## REFERENCES

[1] P. F. Pasquina, B. N. Perry, M. E. Miller, G. S. F. Ling, and J. W. Tsao, "Recent advances in bioelectric prostheses," Neurology: Clinical Practice, vol. 5, no. 2, pp. 164–170, Apr. 2015.

[2] C. G. Bhuvaneswar, L. A. Epstein, and T. A. Stern, "Reactions to Amputation: Recognition and Treatment," The Primary Care Companion to The Journal of Clinical Psychiatry, vol. 09, no. 04, pp. 303–308, 2007.

[3] N. Parajuli, N. Sreenivasan, P. Bifulco, M. Cesarelli, S. Savino, V. Niola, D. Esposito, T. J. Hamilton, G. R. Naik, U. Gunawardana, and G. D. Gargiulo, "Real-Time EMG Based Pattern Recognition Control for Hand Prostheses: A Review on Existing Methods, Challenges and Future Implementation," Sensors, vol. 19, no. 20, p. 4596, 2019.

[4] A. A. Adewuyi, L. J. Hargrove, and T. A. Kuiken, "An Analysis of Intrinsic and Extrinsic Hand Muscle EMG for Improved Pattern Recognition Control," IEEE Transactions on Neural Systems and Rehabilitation Engineering, vol. 24, no. 4, pp. 485–494, May 2015.

[5] Albulbul, Anas. Evaluating Major Electrode Types for Idle Biological Signal Measurements for Modern Medical Technology. MDPI, 24 Aug. 2016, www.ncbi.nlm.nih.gov/pmc/articles/PMC5597189/.

[6] G. Cauwenberghs, Class Lecture, Topic: "Lecture 12 - Biopotential Amplifiers: Problems and Solutions." BENG186B, Department of Bioengineering, University of California San Diego, San Diego, CA., Mar., 18, 2021.

[7] M. Z. Jamal, "Signal Acquisition Using Surface EMG and Circuit Design Considerations for Robotic Prosthesis," in Computational intelligence in Electromyography Analysis – A Perspective on Current Applications and Future Challenges. InTech, 2012, ch.18. Accessed on: March, 18, 2021. [Online]. Available: 10.5772/3315